Theory for Radial Jet Reattachment Flow

R. H. Page,* L. L. Hadden,† and C. Ostowari‡
Texas A&M University, College Station, Texas

The flowfield that develops when a radial jet reattaches to a flat plate is analyzed. Both laminar and turbulent flows are considered. A component analysis is used for the theoretical treatment. The jet flow component is modeled with Schlichting's velocity profile for the laminar case and with Görtler's velocity profile for the turbulent case. The influence of the nozzle exit geometry and the spacing between the radial jet and the flat plate is theoretically determined. The pressure coefficient of the flow immediately below the radial jet nozzle, the flow reattachment angle, and the flow reattachment radius are shown to be dependent on the nozzle exit radius, nozzle exit direction, reattachment plate distance, and laminar or turbulent character of the flow. The equations for the theory are derived, and graphical results are presented.

Nomenclature

b = nozzle width
C_p = pressure coefficient $= p_b - p_\infty/\frac{1}{2}\rho_o U_o$
J = jet momentum per unit perimeter
N_R = nozzle exit Reynolds number $= (\rho U_o b/\mu)$
p_b = pressure immediately below nozzle
p_∞ = atmospheric pressure
Q = volumetric flow per unit perimeter
R_c = radius of curvature of jet path
R_o = dimensionless radial distance at nozzle exit with respect to nozzle width, $= r_o/b$
R_R = dimensionless radial distance at reattachment with respect to nozzle radius, $= r_R/r_o$
r = radial distance from nozzle centerline
s = coordinate along jet path
t = $\tanh(\sigma y_d/s)$(turbulent)
t = $\tanh[0.2752(J/\rho\nu^2)^{1/3}\, y_d/s^{2/3}]$(laminar)
u = local velocity in jet
x = axial distance from center of nozzle exit
y = coordinate perpendicular to jet path
Δ = dimensionless distance to reattachment plate in axial direction with respect to nozzle radius, $= x_p/r_o$
ε_t = virtual kinematic viscosity
θ = flow angle
μ = viscosity
ν = kinematic viscosity
ρ = density
σ = similarity constant for slot jet mixing
Ω = dimensionless distance to reattachment plate along the jet path with respect to nozzle radius, $= s_R/r_o$

Subscripts

b = recirculation region
d = dividing or discriminating streamline location
o = nozzle exit
p = plate
R = reattachment
t = total (i.e., over the entire perimeter)
∞ = atmospheric

Received June 10, 1988; presented as Paper 88-3589 at the 1st National Fluid Dynamics Congress, Cincinnati, OH, July 25-28, 1988; revision received October 14, 1988.

*Forsyth Professor of Mechanical Engineering. Associate Fellow AIAA.
†Aerodynamic Design Engineer, LTV, Dallas, TX. Member AIAA.
‡Associate Professor of Aerospace Engineering. Member AIAA.

Introduction

A SUBMERGED radial jet, as the name implies, represents an axisymmetric radial discharge of a fluid into a free, unbounded atmosphere of the same fluid. Thus, it is a jet that is produced in a radial manner as if it came from a point, finite line source, or a finite cylindrical source. Over the years the radial jet has received little attention in professional literature. This is probably because the centerline velocity of the jet decreases rapidly as the result of both the mixing with the quiescent fluid and the radial expansion with cross-sectional area increase. During the past few years, a group at Texas A&M has taken a fresh look at the radial jet because of interest in its ability to reattach on adjacent surfaces and produce separated-flow patterns of practical benefit.

The practical applications become apparent when one compares the reattaching radial jet to the impinging cylindrical jet. The impinging cylindrical jet usually develops a high-pressure/high heat-transfer region near the centerline of impingement. In contrast, the reattaching radial jet develops a low-pressure/low heat-transfer area near the centerline of impingement but develops a ring of high heat transfer[1] over a somewhat larger area. The combination of low pressure immediately below the nozzle and a high heat-transfer ring leads to industrial applications in which enhanced convective heat transfer is important. Obvious applications also exist in the field of air cushion and VTOL vehicles.

The radial jet was studied by Squire[2] over three decades ago. Heskestad[3] made detailed measurements in a turbulent radial jet over two decades ago. Bourque and Rougier[4] developed a component analysis approach to turbulent annular jet reattachment over one decade ago.

The early theoretical studies by Squire[2] and Schwarz[5] utilized the equations of motion with boundary-layer approximations for a laminar, incompressible, radial free jet. Analytical expressions were drawn from both the velocity and temperature distributions. Heskestad's[3] experimental measurements showed that the velocity profiles in the turbulent radial jet exhibited similarity at various radial locations. Rajaratnam[6] compared the velocity distributions of fully developed flow of the Görtler- and Tollemien-types of solutions with the experimental results of Heskestad. Later, Rodi[7] used a two-equation turbulence model to define the eddy viscosity for an incompressible radial jet. Paully et al.[8] used a standard turbulence model to determine far-field similarity equations for both plane and radial jets. Their results of velocity decay rate, growth rate, and entrainment were found to be consistent with the experimental radial free jet data of Tanaka and Tanaka.[9] Witze and Dwyer[10,11] extensively studied free turbulent radial jets, determining experimentally their spreading

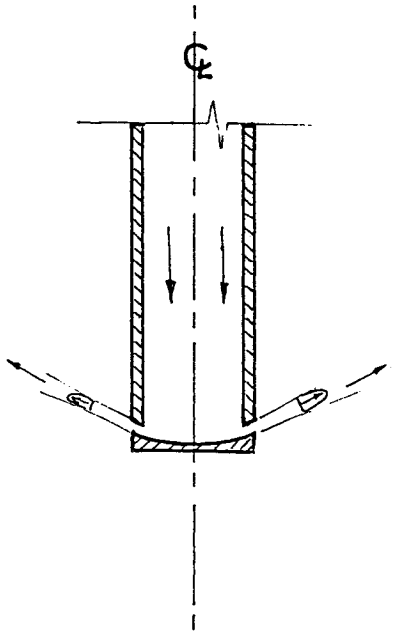

Fig. 1 Free radial jet.

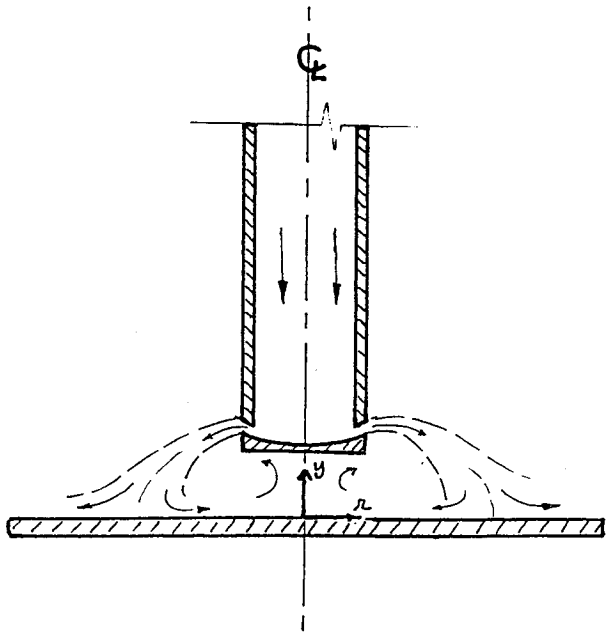

Fig. 2 Radial jet reattachment.

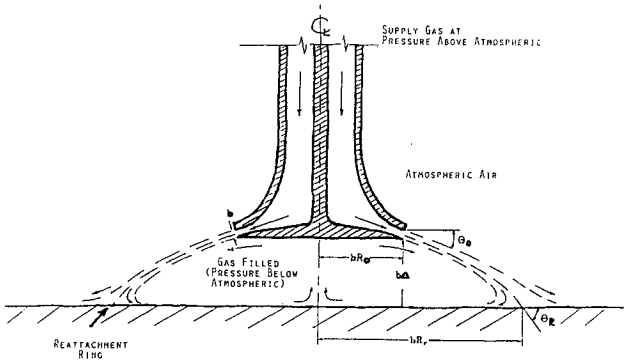

Fig. 3 Schematic of flow.

rates, mean velocity profiles, and relative turbulence intensity profiles. More recently, Wood and Chen[12] presented turbulence model predictions in addition to mean velocity profiles for radial jets using a κ-ϵ turbulence model. All of this past work dealt with a free radial jet. This paper is concerned with the reattachment of a radial jet on a plane surface, i.e., a radial jet that is no longer free but is strongly influenced by an adjacent surface.

The theory presented here is based upon Borque and Rougier's[4] approach to the turbulent annular jet reattachment. It includes a component analysis approach to the laminar radial jet reattachment as well. A radial jet with no surface in its vicinity is illustrated in Fig. 1. Figure 2 illustrates a radial jet with a surface nearby. An overall schematic of the radial jet reattachment is shown in Fig. 3. The plane of the reattachment surface is normal to the centerline of the radial jet delivery tube. The critical geometrical parameters are the angle at which the radial jet leaves the nozzle, the radius of the nozzle, the nozzle exit width, and the spacing of the nozzle from the adjacent surface.

Experimental flow studies of a somewhat similar configuration, where the radial jet was produced by a cylinder protruding from a flat surface, were carried out by Tanaka et al.[13] Experimental studies of the flow, surface heat transfer, and surface pressure distribution of the configuration shown in Fig. 3 were conducted by Ostowari et al.,[14] Ostowari and Page,[15] and Page and Ostowari.[16]

Flow Model

Figure 4 illustrates the flow model. An s, y coordinate system is used for the jet where s is the curvilinear coordinate that follows the centerline of the jet and y is the normal coordinate. The angle that the s coordinate makes with the horizontal continues to change up to reattachment. The flow divides at reattachment with the mass that was mixed in from the recirculation region being turned back toward the centerline while the remaining mass flow is directed out away from the centerline like an axisymmetric radial wall jet.

A local radius of curvature is indicated in Fig. 4. It varies along the path of the jet from nozzle exit to reattachment.

The flow model is made up of various components that are individually analyzed and merged together for the system solution. The following assumptions are made relative to the flow and its components:

1) There is incompressible flow.

2) The exit velocity from the nozzle can be represented by a single value, U_o.

3) The pressure in the recirculation region, p_b, is constant.

4) The jet width is small compared to the radius of curvature of its path and the distance to the radial centerline.

5) Total jet momentum is conserved along the path. Therefore, the momentum per unit perimeter varies with the radius of the jet.

6) The flow at reattachment is essentially two-dimensional, since the jet is thin and the reattachment occurs in a thin layer along the adjacent plate. Furthermore, the velocity profiles of the reverse flow and outward radial flow are assumed to be similar to the parts of the jet profile immediately before the reattachment.

7) For turbulent flow, the jet velocity profile and mass entrainment are given according to Görtler's two-dimensional free jet theory.

8) For laminar flow, the jet velocity profile and mass entrainment are given according to Schlichting's two-dimensional free jet theory.

It has been found experimentally[14] that the pressure in the recirculation region is constant for most geometrical conditions and is, of course, less than the surrounding ambient pressure (i.e., atmospheric pressure). It has also been found from flow visualization studies[17] that the reattachment of the radial jet takes place in a perfectly symmetrical ring with

radial inflow toward the centerline and radial outflow away from the centerline. There was no evidence of variations in the angular directions. Thus, it is appropriate to use a flow model such as that shown in Fig. 4 for the entire region, with the assumption of symmetry around the centerline.

Development of Laminar Theory

In practice, the flow becomes turbulent. Nevertheless, it is instructive to develop the laminar theory, since it provides theoretical limits and the turbulent theory is developed in a very similar way. Schlichting's[18] solution of the two-dimensional laminar jet is utilized. The velocity profile in the s direction was shown to be

$$u = 0.4543(J^2/\rho^2\nu s)^{1/3}\,\mathrm{sech}^2\xi \tag{1}$$

where

$$\xi = 0.2752(J/\rho\nu^2)^{1/3}(y/s^{2/3}) \tag{2}$$

The volume flow per unit perimeter is

$$Q = 2\int_o^\infty u\,\mathrm{d}y = 3.3016(J\nu/\rho)^{1/3}s^{1/3} \tag{3}$$

The rate of entrainment is

$$\frac{\mathrm{d}Q}{\mathrm{d}s} = 1.1005(J\nu/\rho)^{1/3}(s)^{-2/3} \tag{4}$$

The conservation of the total jet momentum yields

$$J2\pi r = J_o 2\pi r_o$$

or

$$J = J_o(r_o/r) \tag{5}$$

where

$$J_o = \rho Q_{ot}^2/b(2\pi r_o)^2 \tag{6}$$

The equation of motion in the y direction relates the pressure difference across the jet to the local radius of curvature of the streamlines. Thus,

$$p_\infty - p_b = J/R_c \tag{7}$$

Since the pressure difference is assumed to be constant and the unit jet momentum varies, the radius of curvature of the path must also vary. Introducing the pressure coefficient and Eq. (5), Eq. (7) becomes

$$R_c/r_o = -2b(C_p r) \tag{8}$$

The rate of entrainment in terms of the total volumetric flow is found from Eqs. (4–6):

$$\mathrm{d}Q = 1.1005\left[\frac{\rho Q_{ot}^2 r_o \nu}{(2\pi r_o)^2 br}\right]^{1/3} s^{-2/3}\,\mathrm{d}s \tag{9}$$

Since $Q_t = 2\pi rQ$, Eq. (9) may be rewritten in dimensionless form as

$$\frac{\mathrm{d}Qt}{Q_{ot}} = 1.1005\left[\frac{2\pi r^2\nu}{Q_{ot}b}\right]^{1/3}\left(\frac{s}{r_o}\right)^{-2/3}\mathrm{d}\left(\frac{s}{r_o}\right) \tag{10}$$

The dimensionless jet path coordinate s/r_o is expressed in terms of dimensionless total volume flow from Eq. (3):

$$(s/r_o)^{2/3} = (Q_t/Q_{ot})^2\left[\frac{Q_{ot}b}{2\pi r^3\nu}\right]^{2/3}(1/3.3016)^2 \tag{11}$$

Substituting Eq. (11) into Eq. (10) yields

$$\frac{\mathrm{d}Q_t}{Q_{ot}}\left(\frac{Q_t}{Q_{ot}}\right)^2 = (1.1005)(3.3016)^2\frac{2\pi r^2\nu}{Q_{ot}b}\,\mathrm{d}\left(\frac{s}{r_o}\right) \tag{12}$$

Equation (12) is prepared for integration by introducing the angle $\theta(\mathrm{d}s = R_c\,\mathrm{d}\theta)$ and Eq. (8). Then,

$$\frac{\mathrm{d}Q_t}{Q_{ot}}\left(\frac{Q_t}{Q_{ot}}\right)^2 = -2(1.1005)(3.3016)^2\frac{2\pi r\nu}{Q_{ot}C_p}\,\mathrm{d}\theta \tag{13}$$

Equation (13) is integrated from the radial jet exit to a station along the jet path, yielding

$$(Q_t/Q_{ot})^3 = 1 - 71.9764(\theta - \theta_o)(2\pi r\nu/C_pQ_{ot}) \tag{14}$$

The location of the dividing streamline is found from its definition,

$$Q_{ot} = 2\pi r\int_{-y_d}^{+y_d} u\,\mathrm{d}y \tag{15}$$

the velocity profile of Eqs. (1) and (2), the conservation of momentum of Eq. (5), and the path coordinate of Eq. (11) as

$$t = \tanh\left[0.2752\left(\frac{J}{\rho\nu^2}\right)^{1/3}\frac{y_d}{s^{2/3}}\right] \tag{16}$$

where

$$t = Q_{ot}/Q_t \tag{17}$$

The momentum equation at reattachment is

$$\int_{-\infty}^{+\infty}\rho u^2\,\mathrm{d}y\cos\theta = \int_{y_d}^{+\infty}\rho u^2\,\mathrm{d}y - \int_{-\infty}^{y_d}\rho u^2\,\mathrm{d}y \tag{18}$$

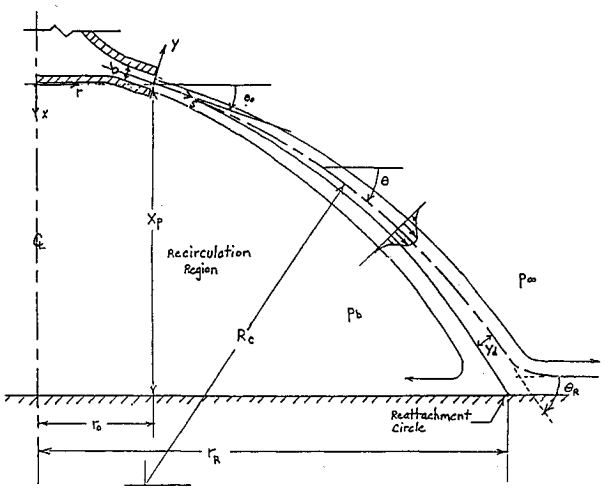

Fig. 4 Flow model geometry.

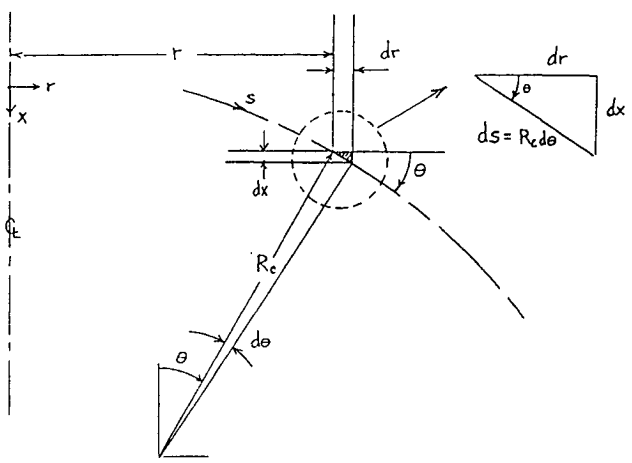

Fig. 5 Jet centerline geometry.

which with Eqs. (3) and (17) becomes

$$\cos\theta = (3t/2) - (t^3/2) \tag{19}$$

The geometry of the jet path is to be determined in terms of x, r, and θ. From Fig. 5 it can be seen that

$$\mathrm{d}(r/r_o) = (R_c/r_o)\cos\theta\ \mathrm{d}\theta \tag{20}$$

$$\mathrm{d}(s/r_o) = (R_c/r_o)\ \mathrm{d}\theta \tag{21}$$

$$\mathrm{d}(x/r_o) = (R_c/r_o)\sin\Theta\ \mathrm{d}\Theta \tag{22}$$

Equations (20–22) can be integrated along the path by using Eq. (8) with the following results:

$$(r/r_o)^2 = 1 - 4b(\sin\theta - \sin\theta_o)/C_p r_o \tag{23}$$

$$\frac{s}{r_o} = \frac{-2b}{C_p r_o}\int_{\theta_o}^{\theta}\frac{\mathrm{d}\theta}{(r/r_o)} \tag{24}$$

$$\frac{x}{r_o} = \frac{-2b}{C_p r_o}\int_{\theta_o}^{\theta}\frac{\sin\theta\ \mathrm{d}\theta}{(r/r_o)} \tag{25}$$

A set of equations sufficient to determine the flow structure now exists by using the total volume flow (14), the dividing streamline (17), the momentum balance (19), and Eqs. (23–25) identifying the path line location. For convenience they are repeated here in dimensionless form with the Reynolds number introduced:

$$(Q_t/Q_{ot})^3 = 1 - 71.9764(R_R/N_R C_p)(\theta_R - \theta_o) \tag{26}$$

$$y_d/r_o = \frac{1}{0.2752}\left(\frac{\Omega^2 R_R}{N_R^2 R_o}\right)^{1/3}\tanh^{-1}t \tag{27}$$

$$\cos\theta_R = (3t_R/2) - (t_R^3/2) \tag{28}$$

$$R_R^2 = 1 - 4(\sin\theta_R - \sin\Theta_o)/R_o C_p \tag{29}$$

$$\Omega = \frac{-2}{C_p R_o}\int_{\theta_o}^{\theta_R}\frac{\mathrm{d}\theta}{R_R} \tag{30}$$

$$\Delta = \frac{-2}{C_p R_o}\int_{\theta_o}^{\theta_R}\frac{\sin\theta\ \mathrm{d}\theta}{R_R} \tag{31}$$

Development of Turbulent Theory

Using the same flow model as that used for the laminar case, a turbulent jet mixing component is introduced. Following the approach of Bourque and Rougier,[4] we utilized Görtler's[19] two-dimensional jet mixing solution. This introduces the empirical constant σ, which is also called the spread parameter or similarity constant. Values for the spread parameter have been determined experimentally by many investigators. They range from 7.67 obtained by Reichardt[20] to 15 obtained by Sawyer.[21] The velocity profile is represented by the following equation:

$$u = 0.8660(J\sigma/\rho s)^{1/2}\,\mathrm{sech}^2\eta \tag{32}$$

where

$$\eta = \sigma y/s \tag{33}$$

The volume flow per unit perimeter is

$$Q = 1.732(J/\rho\sigma)^{1/2}s^{1/2} \tag{34}$$

The rate of entrainment is

$$\frac{\mathrm{d}Q}{\mathrm{d}s} = 0.8660(J/\rho\sigma)^{1/2}s^{-1/2} \tag{35}$$

Using Eq. (6) for the conservation of total jet momentum, the rate of total entrainment becomes

$$\frac{\mathrm{d}Q_t}{Q_{ot}} = 0.8660(r/\sigma b)^{1/2}(s/r_o)^{-1/2}\,\mathrm{d}(s/r_o) \tag{36}$$

Equation (34) is expressed in terms of r_o and total flows as

$$\left(\frac{s}{r_o}\right)^{1/2} = \frac{Q_t}{Q_{ot}}(\sigma b/3r)^{1/2} \tag{37}$$

Equation (37) is substituted into Eq. (36), which yields

$$\frac{Q_t}{Q_{ot}}\frac{\mathrm{d}Q_t}{Q_{ot}} = \frac{3}{2}\frac{1}{\sigma}\frac{r}{b}\,\mathrm{d}\left(\frac{s}{r_o}\right) \tag{38}$$

The geometrical relation $\mathrm{d}s = R\ \mathrm{d}\theta$ and Eq. (8) simplify Eq. (38) to

$$\frac{\mathrm{d}Q_t}{Q_{ot}}\frac{Q_t}{Q_{ot}} = (-3/\sigma C_p)\ \mathrm{d}\theta \tag{39}$$

Equation (39) is integrated to provide the following volume flow equation for the turbulent radial jet:

$$\left(\frac{Q_t}{Q_{ot}}\right)^2 = 1 - (6/\sigma C_p)(\theta - \theta_o) \tag{40}$$

The equation that identifies the dividing streamline is derived in the same manner as for laminar flow and is given by

$$Q_{ot}/Q_t = t = \tanh(\sigma y_d/s) \tag{41}$$

The equation relating t and θ is again obtained by the momentum balance equation and is the same as Eq. (19).

The equations describing the geometry of the turbulent flow radial jet are the same as for the laminar flow, i.e., Eqs. (20–25). Thus, it can be seen that the equations for the turbulent flow are very similar to those for the laminar theory with the exception of the volume flow equation and the equation for the dividing streamline location. The characteristic parameter for the turbulent flow equations is the spreading parameter σ, whereas the characteristic parameter for the laminar flow equations is the nozzle exit Reynolds number.

Results from Theory

A computer program was developed to solve simultaneously the components of the theoretical analysis. The integrals present in the reattachment distance equations were solved by numerical integration using a 32-point Gauss quadrature formula. The pressure coefficient, reattachment angle, and reattachment radius were chosen as the dependent

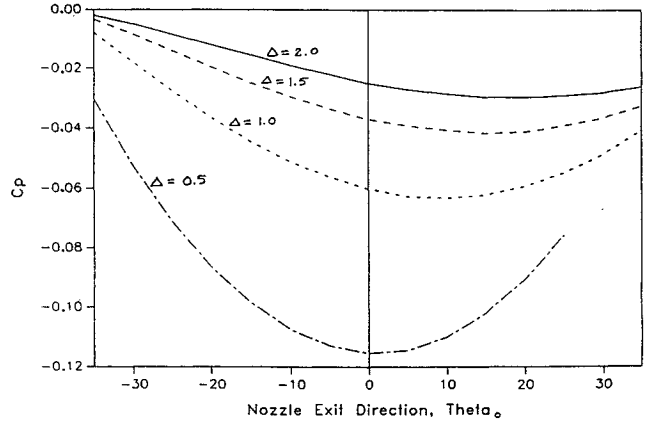

Fig. 6 Laminar pressure coefficient ($R_o = 8$, $N_R = 10$).

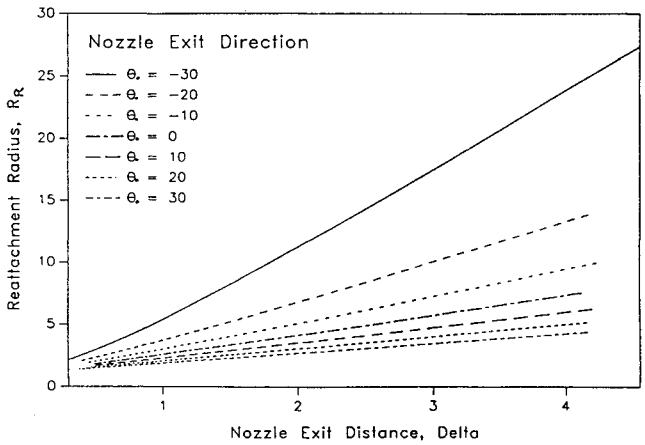

Fig. 7 Laminar reattachment radius ($R_o = 8$, $N_R = 10$).

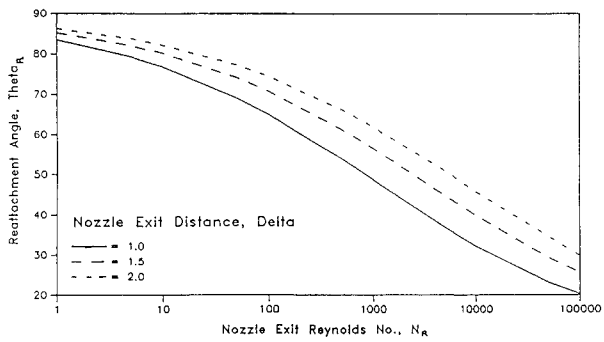

Fig. 8 Laminar reattachment angle ($R_o = 8$, $\theta_o = 0$).

variables. The formulation for the laminar case is summarized functionally as

$$C_p = C_p(\theta_o, R_o, N_R, \Delta) \tag{42}$$

$$\theta_R = \theta_R(\theta_o, R_o, N_R, \Delta) \tag{43}$$

$$R_R = R_R(\theta_o, R_o, N_R, \Delta) \tag{44}$$

The formulation for the turbulent case is summarized functionally as

$$C_p = C_p(\theta_o, R_o, \Delta, \sigma) \tag{45}$$

$$\theta_R = \theta_R(\theta_o, R_o, \Delta, \sigma) \tag{46}$$

$$R_R = R_R(\theta_o, R_o, \Delta, \sigma) \tag{47}$$

Typical theoretical results are shown in the following figures. Figures 6–8 were derived from laminar flow calculations. Figure 6 illustrates the strong influence of the radial nozzle exit angle on the pressure coefficient. It should be recalled that positive nozzle exit angles indicate that the radial jet is turning toward the reattachment plate. Also note that, as one would expect, the spacing between the radial nozzle and the plate has a strong influence on the pressure coefficient. Figures 6 and 7 were calculated for a nozzle Reynolds number of 10. Figure 7 illustrates the dependence of the reattachment radius on the nozzle exit distance. It is, of course, a linear relationship for a fixed nozzle exit angle. Figure 8 was calculated for a dimensionless nozzle radius of 8 and an initial radial jet angle of 0 deg. The nozzle exit Reynolds number is shown on a logarithmic scale. In practice, such large Reynolds numbers would be impossible to obtain before transition occurred. Nevertheless, this figure serves to show the theoretical limit that as the Reynolds number approaches infinity

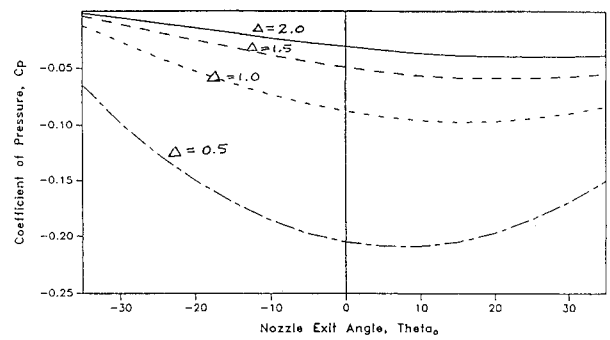

Fig. 9 Turbulent pressure coefficient ($R_o = 8$, $\sigma = 10$).

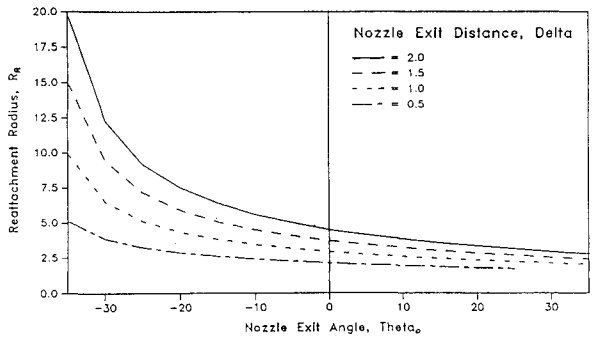

Fig. 10 Turbulent reattachment radius ($R_o = 8$, $\sigma = 10$).

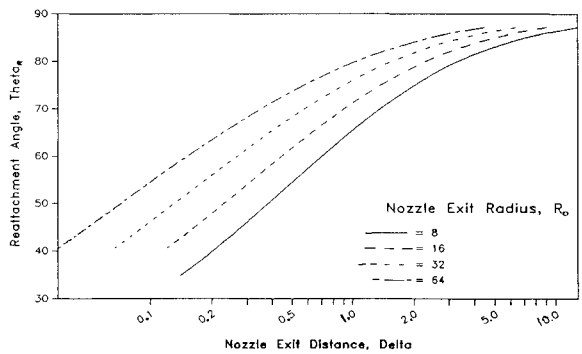

Fig. 11 Turbulent reattachment angle ($\theta_o = 0$, $\sigma = 10$).

(and thus the viscosity approaches zero), the reattachment angle must return to 0 deg, since the viscous effects are disappearing.

Figures 9–11 were calculated for turbulent conditions. In all cases, Görtler's similarity parameter σ was set equal to 10. Figures 9 and 10 were determined for a dimensionless nozzle radius of 8. Figure 9 shows the strong effect of the nozzle exit

Table 1 Comparison of experiment with theory

Geometry			Experiment		Theory	
Θ_o	R_o	Δ	C_p	R_R	C_p	R_R
−10	18	0.50	−0.023	1.99	−0.046	2.16
0	18	0.25	−0.056	1.56	−0.078	1.55
0	18	0.50	−0.025	1.81	−0.050	1.94
0	6	0.50	−0.064	1.91	−0.080	2.21
0	6	1.00	−0.031	2.76	−0.048	3.04
10	9	0.50	−0.041	1.72	−0.061	1.91
10	9	1.00	−0.022	2.41	−0.040	2.55

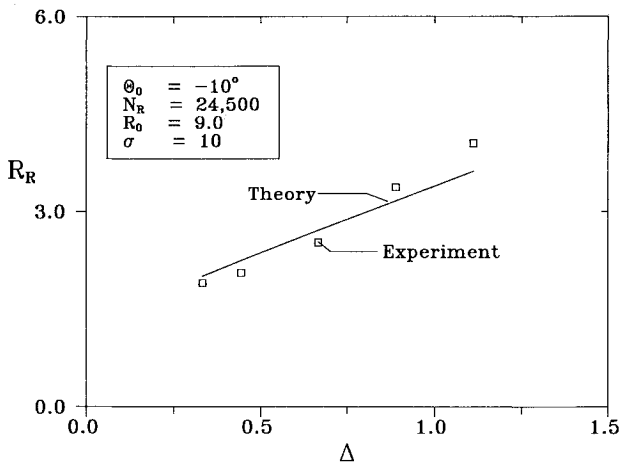

Fig. 12 Turbulent reattachment radius (theory and experiment).

angle and reattachment plate spacing on the pressure coefficient. It can be observed that slightly positive exit angles give the minimum values for the pressure coefficient. Figure 10 illustrates the effects of the exit angle on the reattachment radius. Figure 11 was calculated for a fixed exit angle of 0 deg and illustrates the strong turning that takes place in the radial jet. The reattachment angles are plotted vs the spacing between the plate. Note that even small values of plate spacing Δ produce rather large reattachment angles. The theoretical results for the turbulent case have been shown[22] to be in good agreement with our experimental data on pressures and reattachment locations of reattaching radial jets.

Table 1 illustrates the agreement between theory and our 1988 experiments with varying initial angle of the radial jet. The theory was calculated with $\sigma = 24$, a value sometimes used for curved-slot jets. The theory predicts the trends correctly, but the pressure coefficients have a large disparity when R_o is large. Figure 12 illustrates the good agreement of the 1988 data with the theory for the location of the reattachment radius.

Conclusions

A theory has been derived for the laminar and turbulent flow calculation of the flowfield that develops when a radial jet attaches to an adjacent flat surface that is normal to the centerline of the radial jet. The theory permits the determination of the low pressure in the region immediately below the radial jet as well as the geometry of the reattachment. Significant curvature of the reattaching jet is predicted.

Acknowledgment

This research was partially funded by the National Science Foundation under Grant CBT-8418493.

References

[1]Ostowari, C., Paikert, B., and Page, R. H. "Heat Transfer Measurements of Radial Jet Reattachment on a Flat Plate," *Proceedings of National Fluid Dynamics Congress*, Vol. III, AIAA, Washington, D.C., 1988, pp. 1901–1907.

[2]Squire, H. B., "Radial Jets," 50 *Jahre Grenzschichtforschung*, Vieweg & Sons, Braunschweig, FRG, 1955, pp. 47–54.

[3]Heskestad, G., "Hot Wire Measurements in a Radial Turbulent Jet," *Journal of Applied Mechanics*, Vol. 88, 1966, pp. 417–424.

[4]Bourque, C. and Rougier, P., "Annular Jet Reattachment," *Transactions of CSME*, Vol. 2, No. 2, 1973, pp. 105–113.

[5]Schwarz, W. H., "The Radial Free Jet," *Chemical Engineering Science,* Vol. 18, 1963, pp. 50–62.

[6]Rajaratnam, N., *Turbulent Jets*, Elsevier Scientific Publishing, New York, 1976, pp. 50–62.

[7]Rodi, W., "The Prediction of Free Turbulent Boundary Layers by Use of a Two-Equation Model of Turbulence," Ph.D. Thesis, University of London, England, 1972.

[8]Paully, A. J., Melnick, R. E., Rubel, A., Rudman, S., and Siclairi, M. J., "Similarity Solutions for Plane and Radial Jets Using a Kapa-Epsison Turbulence Model," American Society of Mechanical Engineers, Paper 84-WA/FE-3, 1984.

[9]Tanaka, T. and Tanaka, E., "Experimental Study of a Radial Turbulent Jet," *Bulletin of the Japan Society of Mechanical Engineers*, Vol. 19, 1976, pp. 792–799.

[10]Witze, P. O. and Dwyer, H. A., "The Turbulent Radial Jet," *Journal of Fluid Mechanics*, Vol. 75, Pt. 3, June 1976, pp. 401–417.

[11]Witze, P. O. and Dwyer, H. A., "Impinging Axisymmetric Turbulent Flows: The Wall Jet, the Radial Jet and Opposing Free Jets," *Proceedings of the Symposium on Turbulent Shear Flows*, Pennsylvania State University, University Park, PA, 1977, p. 2.33–2.4.

[12]Wood, P. E. and Chen, C. P., "Turbulence Model Predictions of the Radial Jet—A Comparison of Kappa-Epsilon Models," *Journal of Chemical Engineering*, Vol. 63, No. 2, April 1985, pp. 177–182.

[13]Tanaka, T., Tanaka, E., and Naganuma, N., "5th Report, Attaching Flow From an Inclined Nozzle on an Adjacent Offset Disk Plate," *Bulletin of the JSME*, Vol. 24, No. 187, 1981, p. 82 (this report includes the references to the earlier Tanaka reports).

[14]Ostowari, C., Page, R. H., and MacGregor, J. D., III, "Heat Transfer in a Reattaching Radial Jet Flow," *Proceedings of the 2nd ASME/JSME Joint Thermal Engineering Conference*, American Society of Mechanical Engineering, New York, 1987, pp. 455–459.

[15]Ostowari, C. and Page, R. H., "Flow Features of a Radial Jet," *Proceedings of 11th Canadian Congress of Applied Mechanics*, University of Alberta, Edmonton, Canada, June 1987.

[16]Page, R. H. and Ostowari, C., "Heat Transfer During a Radial Jet Reattachment," *Proceedings of Symposium on Heat and Mass Transfer*, University of Illinois at Urbana-Champaign, Department of Mechanical and Industrial Engineering, Urbana, IL, Oct. 1987, pp. 1–16.

[17]Page, R. H., Ostowari, C., and Carbone, J. S., "Radial Jet Flow," *Proceedings of the 4th International Symposium on Flow Visualization*, Hemisphere Publishing Co., NY, Aug. 1986, pp. 513–521.

[18]Schlichting, H., "Laminar Strahlausbreitung," *Zeitschrift fuer Angewandte Math. u. Mech.*, Vol. 13, Aug. 1933, p. 260.

[19]Görtler, H. "Berechnung von Aufgaben der freien Turbulenz auf Grund eines neuen. Näherungsansatzes," *Zeitschrift fuer Angewandte Math. u. Mech.*, Vol. 22, Oct. 1942, pp. 244–254.

[20]Reichardt, H., "Gesetzmäsigkeiten der frein Turbulenz," *VDI—Forschungsheft*, Vol. 414, 1942.

[21]Sawyer, R. A., "The Flow Due to a Two-Dimensional Jet Issuing Parallel to a Flat Plate," *Journal of Fluid Mechanics*, Vol. 9, Pt. 4, Dec. 1960, pp. 543–561.

[22]McGregor, J. D. III, "An Experimental Study of Radial Jet Reattachment on a Flat Plate," M.S. Thesis, Mechanical Engineering Dept., Texas A&M University, College Station, TX, 1986.